Embedded-atom models of 12 cubic metals incorporating second- and third-order elastic-moduli data

Somchart Chantasiriwan* and Frederick Milstein
Departments of Materials and Mechanical Engineering, University of California, Santa Barbara, California 93106
(Received 7 October 1997)

An embeded-atom method (EAM) formulation that can reproduce identically the empirically determined second-order and third-order elastic moduli is employed in constructing the EAM models of 12 cubic metals (Ag, Al, Au, Cu, Fe, K, Li, Mo, Na, Nb, Ni, and Rb). The models yield phase stabilities, pressure-volume curves, and phonon-frequency spectra that are in generally good agreement with experiments. [S0163-1829(98)00630-4]

I. INTRODUCTION

The embedded-atom method (EAM) has been widely used in the study of condensed matter; Ref. 1 contains a comprehensive review. Chantasiriwan and Milstein[2] recently examined the higher-order elasticity of cubic metals in the framework of the EAM. They developed formulas for computing the third-order elastic moduli (TOEM) in general EAM formulations and showed that appropriate groupings of the elastic moduli depend solely on either the electron-density function or the pair-potential function. Their aim, in part, was to develop a convenient method of constructing EAM models that incorporate experimental values of both the second-order elastic moduli (SOEM) and the TOEM; such models thereby display accurately the harmonic and anharmonic, anisotropic, elastic behavior of the parent crystal. As examples of the efficacy of that approach, specific EAM models were constructed for four metals (i.e., aluminum, copper, sodium, and molybdenum). These models identically reproduced the respective second- and third-order elastic moduli, as well as the binding energy, atomic volume, unrelaxed vacancy formation energy, and Rose's universal equation of state. They also provided reasonable phonon-frequency spectra and structural energy differences.

In the present paper we modify the EAM formulation of Ref. 2 in order to improve the fit between the theoretical and experimental pressure-volume relations. In addition, the formulation is used to construct specific EAM models for 12 metals (Ag, Al, Au, Cu, Fe, K, Li, Mo, Na, Nb, Ni, and Rb). All of the SOEM (C_{11}, C_{12}, and C_{44}) and TOEM (C_{111}, C_{112}, C_{123}, C_{144}, C_{166}, and C_{456}) of each model are identical with those empirically determined for the metal itself (all elastic-moduli data are experimental with the exceptions of the TOEM of the alkali metals Li, Na, K, and Rb, which were taken from pseudopotential calculations because experimental values of these TOEM were not found in the literature). The theoretical and experimental pressure-volume (P-V) and phonon-dispersion relations of each metal are also compared; there is excellent agreement among the respective P-V relations and, as in Ref. 2, reasonably good agreement among the phonon relations.

It is our intention, in due course, to use these EAM models to explore the theoretical elastic response of metals at finite strain, including theoretical strengths,[3–5] elastic stability under load,[5–8] and bifurcations leading from primary to secondary crystallographic configurations under prescribed modes of loading.[9–11] An accompanying paper uses the models to examine and compare the theoretical responses of the metals to uniaxial loading.

II. MODIFIED EQUATION OF STATE

In the EAM format, the cohesive energy per atom E of a homogeneous monatomic crystal can be written as

$$E=F(\rho)+\tfrac{1}{2}\sum_j \phi(r_j), \tag{1a}$$

with

$$\rho=\sum_j f(r_j), \tag{1b}$$

where the summations are performed over all atoms except the reference atom in the crystal, and r_j is the distance between the reference atom and a surrounding atom j. Here, we use the same forms for the pair potential $\phi(r)$ and the electron-density function $f(r)$ as in Ref. 2; these are repeated below as Eqs. (2) and (3);

$$\phi(r)=A(r-r_m)^4[1+d_1r+d_2r^2+d_3r^3+d_4r^4+d_5r^5+d_6r^6], \tag{2}$$

where r_m is the cutoff distance [i.e., $\phi(r)\equiv 0$ for $r\geqslant r_m$], and A and the d_i are fitting parameters that are determined from empirical values of the atomic volume V_0 at zero pressure, the unrelaxed vacancy formation energy E_{IV}, and the combinations of elastic moduli $C_{11}-C_{12}$, C_{44}, $C_{111}-3C_{112}+2C_{123}$, $C_{144}-C_{166}$, and C_{456};[2] the analytic expressions for these quantities are given in Eqs. (24)–(30) in Ref. 2. The cutoff distance r_m must be greater than the third-nearest-neighbor distance in order to avoid artificial restrictions on the calculated values of the C_{ijk}, e.g., $C_{144}=C_{166}$ for bcc and $C_{456}=0$ for fcc.[2] With regard to $f(r)$, Chantasiriwan and Milstein have demonstrated theoretically the importance of selecting an oscillatory form; the following was found to be suitable:

TABLE I. The physical constants of Ag, Al, Au, Cu, Fe, K, Li, Mo, Na, Nb, Ni, and Rb used as input parameters for EAM model construction. Data for the elastic moduli and the lattice constants are for room temperature, except for K, Li, Na, and Rb, which are for low temperature.

	Ag	Al	Au	Cu	Fe	K	Li	Mo	Na	Nb	Ni	Rb
a_0 (Å)[a]	4.10	4.03	4.09	3.60	2.87	5.25	3.49	3.15	4.23	3.31	3.52	5.62
E_{IV} (eV)	1.1[b]	0.66[c]	0.9[b]	1.28[b]	1.79[d]	0.42[e]	0.34[f]	3.1[g]	0.42[h]	2.75[g]	1.6[i]	0.312[j]
$E_{\rm coh}$ (eV)[k]	2.95	3.34	3.81	3.50	4.29	0.941	1.65	6.81	1.13	7.47	4.45	0.852
C_{11} (Mbar)[a]	1.222	1.143	1.929	1.762	2.26	0.0416	0.148	4.696	0.0821	2.465	2.508	0.0296
C_{12} (Mbar)[a]	0.907	0.6192	1.638	1.2494	1.40	0.0341	0.125	1.676	0.0683	1.333	1.500	0.0244
C_{44} (Mbar)[a]	0.454	0.3162	0.415	0.8177	1.16	0.0286	0.108	1.068	0.0577	0.284	1.235	0.016
C_{111} (Mbar)	−8.43[l]	−14.27[m]	−17.30[l]	−20.0[l]	−27.2[n]	−0.387[o]	−2.70[o]	−35.57[p]	−0.935[o]	−25.64[q]	−20.4[r]	−0.274[o]
C_{112} (Mbar)	−5.29	−4.08	−9.22	−12.2	−6.08	−0.057	−0.386	−13.33	−0.144	−11.40	−10.3	−0.041
C_{123} (Mbar)	1.89	0.32	−2.33	−5.0	−5.78	−0.091	−0.693	−6.17	−0.230	−4.67	−2.1	−0.059
C_{144} (Mbar)	0.56	−0.85	−0.13	−1.32	−8.36	−0.114	−0.944	−2.69	−0.298	−3.43	−1.4	−0.075
C_{166} (Mbar)	−6.37	−3.96	−6.48	−7.05	−5.3	−0.058	−0.590	−8.93	−0.172	−1.677	−9.2	−0.035
C_{456} (Mbar)	0.83	−0.42	−0.12	0.25	−7.2	−0.097	−0.733	−5.55	−0.248	1.366	−0.7	−0.069

[a]Reference 15.
[b]Reference 16.
[c]Reference 17.
[d]Reference 18.
[e]Reference 19.
[f]Reference 20.
[g]Reference 21.
[h]Reference 22.
[i]Reference 23.
[j]Reference 24.
[k]Reference 25.
[l]Reference 26.
[m]Reference 27.
[n]Reference 28.
[o]Reference 29.
[p]Reference 30.
[q]Reference 31.
[r]Reference 32.

$$f(r)=\frac{1+b_1\cos(\alpha r)+b_2\sin(\alpha r)}{r^{\beta}}, \tag{3}$$

where α and β are positive parameters, and b_1 and b_2 are fitting parameters that are chosen to satisfy the expressions for the elastic-moduli ratios $(C_{12}-C_{44})/(C_{144}-C_{456})$ and $(C_{12}-C_{44})/(2C_{144}+C_{112}-C_{166}-C_{123}-C_{456})$ [see Eqs. (22) and (23) in Ref. 2].

The primary difference between the EAM formulation used here and that of Ref. 2 lies in the embedding function $F(\rho)$. Previously, we used Rose's universal equation of state[12] to determine $F(\rho)$, following the suggestion of Foiles, Baskes, and Daw.[13] For a cubic crystal with lattice parameter a, Rose's equation of state (EOS) is

$$E_{\rm EOS}(a^*)=-E_{\rm coh}(1+a^*+ka^{*3})e^{-a^*} \tag{4}$$

with $a^*=(a-a_0)/a_0\lambda$ and $\lambda=\sqrt{E_{\rm coh}/9V_0\kappa}$. Substitution of the energy $E_{\rm EOS}$ for the cohesive energy E in Eq. (1a) yields

$$F(\rho)=E_{\rm EOS}(a^*)-\tfrac{1}{2}\sum_j \phi(r_j). \tag{5}$$

The constants a_0, $E_{\rm coh}$, V_0, and κ are the lattice parameter, magnitude of cohesive energy, volume per atom, and bulk modulus, respectively, at the unstressed reference state. The numerical value of k, which clearly influences the curvature of the theoretical P-V relation, was set equal to 0.05 by Rose *et al.*[12] from thermal expansion data of Cu. In Ref. 2, we determined values of k based on the pressure derivative of the bulk modulus κ', evaluated from SOEM and TOEM data, as discussed below. [We refer to Eq. (4) as ''Rose's EOS'' regardless of the value of k.] Since $P=-dE/dV$ and $\kappa=V\,d^2E/dV^2$,

$$\kappa'=\frac{d\kappa}{dP}=\frac{d\kappa/dV}{dP/dV}=\frac{-V\,d^3E/dV^3}{d^2E/dV^2}-1, \tag{6}$$

where the derivatives are taken at $P=0$. Evaluation of Eq. (6) using Eq. (4) yields

$$k=\frac{\lambda(\kappa'-1)}{2}-\frac{1}{3}, \tag{7}$$

wherein κ' is computed from[14]

$$\kappa'=-\frac{C_{111}+6C_{112}+2C_{123}}{3(C_{11}+2C_{12})}. \tag{8}$$

For example, from the data in Table I, Eqs. (7) and (8) give $k=0.130$, 0.353, −0.004, and 0.032 for Al, Cu, Na, and Mo, respectively. However, as seen in Fig. 1, neither these values nor $k=0.05$ consistently provides very good fits to the experimental P-V data at very high pressures. On the other hand, the respective values of $k=0.03$, 0.06, 0.00, and −0.05 improve the appearance of the P-V correspondences of these metals at high pressures, but these values do not satisfy the elastic-moduli relations (7) and (8). Thus, for modeling cubic metals, the use of Rose's EOS (without modification) to obtain good agreement with P-V data and the use of SOEM and TOEM to obtain good anisotropic elastic behavior are somewhat incompatible. In view of this consideration, we have adopted a simple modification to the EOS that enables the curvature of the P-V relation at $P=0$ to agree with Eq.

(8), while also yielding agreement with Rose's EOS at intermediate and large compressions and expansions. This modified EOS is as follows:

$$\tilde{E}_{\mathrm{EOS}}(a)=\begin{cases} -E_{\mathrm{coh}}(1+a^*+ka^{*3})e^{-a^*} & \text{for } a/a_0\leqslant 0.95 \text{ or } a/a_0\geqslant 1.05 \\ -E_{\mathrm{coh}}+\omega_1\left(\dfrac{a}{a_0}-1\right)^2+\omega_2\left(\dfrac{a}{a_0}-1\right)^3+\displaystyle\sum_{i=1}^{4}\gamma_i\left(\dfrac{a}{a_0}-1\right)^{i+3} & \text{for } 0.95<a/a_0\leqslant 1 \\ -E_{\mathrm{coh}}+\omega_1\left(\dfrac{a}{a_0}-1\right)^2+\omega_2\left(\dfrac{a}{a_0}-1\right)^3+\displaystyle\sum_{i=1}^{4}\eta_i\left(\dfrac{a}{a_0}-1\right)^{i+3} & \text{for } 1<a/a_0<1.05\,. \end{cases} \tag{9}$$

With this EOS, at $P=0$ $(a/a_0=1)$,

$$\kappa=\frac{2\omega_1}{9V_0}, \tag{10}$$

and

$$\kappa'=1-\frac{\omega_2}{\omega_1}, \tag{11}$$

so $\omega_1=1.5V_0(C_{11}+2C_{12})$ and $\omega_2=0.5V_0(C_{111}+6C_{112}+2C_{123})+\omega_1$; these relations are used to compute ω_1 and ω_2, thus satisfying Eq. (8). At high compressions and expansions ($a/a_0\leqslant 0.95$ and $a/a_0\geqslant 1.05$), Rose's EOS is identically satisfied; a^* is as defined in Eq. (4) and k is chosen to fit the P-V data. In order to ensure correspondence with Rose's EOS at intermediate lattice compressions and expansions, the parameters γ_i and η_i $(i=1-4)$ are determined from the requirement of continuity of $\tilde{E}_{\mathrm{EOS}}$ and its first three derivatives at $a/a_0=0.95$ and 1.05; i.e., the series expansions used to specify the EOS in the range $0.95<a/a_0<1.05$ are matched to Rose's EOS at $a/a_0=0.95$ and 1.05. The embedding function F is then determined from

$$F(\rho)=\tilde{E}_{\mathrm{EOS}}(a)-\tfrac{1}{2}\sum_j \phi(r_j). \tag{12}$$

III. EAM MODEL PARAMETERS

In this section, the construction of the EAM models for seven bcc metals (Fe, K, Li, Mo, Na, Nb, and Rb) and five fcc metals (Ag, Al, Au, Cu, and Ni) is described in detail. Three distinct groups of parameters are determined from solutions of simultaneous equations and the quality of the theoretical P-V and phonon-dispersion relations; these groups are the following. (1) The parameters in $\tilde{E}_{\mathrm{EOS}}$ are k, η_i, and γ_i (i goes from 1–4). (2) The parameters in $f(r)$ are α, β, b_1, and b_2. (3) The parameters in $\phi(r)$ are r_m, A, and d_i (i goes from 1–6). The construction of the EAM models is simplified because the parameters in each group are independent of those in the other two groups. In the manner of Ref. 2, the input data used in the construction of the current EAM models are the lattice constant, the cohesive energy, the unrelaxed vacancy formation energy, the three second-order elastic moduli, and the six third-order elastic moduli (see Table I). These quantities are fit identically to the models.

In order to determine the parameters in the first group, theoretical P-V relations based on Rose's EOS are computed and compared with experimental results. For each metal, the value of k that yields good agreement between theory and experiment at high pressures is selected. Once k is known, the parameters η_j and γ_j are fit to Rose's EOS as described in the previous section.

While determining the fitting parameters in the second group, α and β were initially treated as ''free parameters,'' and the values of b_1 and b_2 were computed from Eqs. (22) and (23) in Ref. 2. It was observed that the values of α and β were subject to certain restrictions, which result from the requirement that $\rho(a)$, as calculated from the lattice summation in Eq. (1b), must be a single-valued function of a. This requirement, which is evident from Eq. (5), was found to be satisfied for each metal, for a particular range of values of α. The size of this range varies inversely with β, and the range may vanish as β increases. From a computational viewpoint, it is desirable for β to be sufficiently large to make $f(r)$ a short-ranged function, yielding rapid convergence of the lattice summations. A nonvanishing range of appropriate α values was found for each metal for $\beta=10$; we thus settled upon this value of β. Initially, several values of α were ''tried'' for a number of metals. It was found that the numerical value of α did not influence the phonon-frequency spectra or the mechanical response of the model strongly; so we arbitrarily chose α to be a whole number in the range.

Finally, for selected values of r_m, the remaining parameters in $\phi(r)$ were determined uniquely from Eqs. (24)–(30) in Ref. 2. The main criteria employed in the selection of the final values of r_m were (i) the calculated differences between the energies of the fcc and the bcc structures, $\Delta E=E_{\mathrm{fcc}}-E_{\mathrm{bcc}}$, should be positive for the metals Fe, K, Mo, Nb, and Rb and negative for Ag, Al, Au, Cu, Li, Na, and Ni, at zero pressure, in conformance with experimental information on phase stability, and (ii) the theoretical phonon-dispersion curves should be ''optimal'' when compared with experiment. Additional criteria were set for the metals Fe, K, Na, and Rb, which undergo phase transformations under pressure.[33] That is, for these metals, (i) the theoretical fcc-bcc free-energy difference, $\Delta G=\Delta E+P\Delta V$ (where ΔV is the difference between the theoretical fcc and bcc atomic volumes at pressure P), should change sign, with increasing pressure, from positive to negative for Fe, K, and Rb and from negative to positive for Na, and (ii) the theoretical values of pressure at which the respective values of ΔG vanish should be of the same order of magnitude as the experimentally observed phase transition pressures.

TABLE II. Parameters of model EAM functions for 12 metals. The unit of A is eV/Å^4 and the unit of d_n is Å^{-n}.

	Ag	Al	Au	Cu
γ_1 (eV)	14 495.346 52	−3989.565 406	9445.865 571	−17 259.616 81
γ_2 (eV)	395 465.8578	−132 139.8801	229 182.9206	−541 086.9574
γ_3 (eV)	5 312 561.379	−1 753 510.429	3 105 624.331	−7 195 460.939
γ_4 (eV)	26 534 316.50	−8 771 590. 264	15 493 942.00	−35 988 498.49
η_1 (eV)	−12 046.123 28	4781.276 350	−6056.628 891	18 726.460 78
η_2 (eV)	395 472.2278	−132 139.3587	229 190.6785	−541 085.045
η_3 (eV)	−5 304 003.255	1 754 827.731	−3 095 343.756	7 198 976.218
η_4 (eV)	26 536 845.88	−8 771 382.584	15 497 019.75	−35 987 737.82
k	0.11	0.03	0.02	0.06
r_m (Å)	5.50	6.70	5.28	4.50
A	14.908 064 49	−0.321 538 123 4	−60.069 286 29	25.046 204 27
d_1	−1.703 063 442	−1.971 137 745	−1.840 544 567	−2.098 826 585
d_2	1.206 516 952	1.520 390 482	1.400 563 316	1.840 347 959
d_3	−0.454 778 800 8	−0.595 330 310 0	−0.564 392 065 7	−0.860 411 610 8
d_4	$9.610\,249\,944\times10^{-2}$	0.125 730 889 2	0.127 123 719 1	0.225 611 227
d_5	$-1.078\,577\,47\times10^{-2}$	$-1.361\,835\,637\times10^{-2}$	$-1.518\,586\,139\times10^{-2}$	$-3.140\,081\,975\times10^{-2}$
d_6	$5.017\,307\,440\times10^{-4}$	$5.914\,217\,027\times10^{-4}$	$7.522\,881\,932\times10^{-4}$	$1.808\,853\,498\times10^{-3}$
β	10	10	10	10
α (Å^{-1})	6	4	4	7
b_1	0.239 827 315 4	0.310 473 843 3	0.461 170 630 4	0.111 910 600 4
b_2	$-7.281\,818\,261\times10^{-2}$	0.487 991 625 4	0.197 522 660 9	0.245 285 818 2
	Fe	K	Li	Mo
γ_1 (eV)	−3362.890 156	652.149 575 9	−2496.393 012	−13 576.835 45
γ_2 (eV)	−119 251.2897	18 463.193 62	−75 600.013 99	−437 305.7752
γ_3 (eV)	−1 578 535.082	246 553.7779	−1 007 811.084	−5 822 805.449
γ_4 (eV)	−7 897 739.845	1 232 713.383	−5 039 077.496	−29 107 989.53
η_1 (eV)	4533.986 271	−580.560 779 8	2542.685 291	15 534.391 49
η_2 (eV)	−119 250.7307	18 463.186 31	−75 600.015 72	−437 309.6601
η_3 (eV)	1 580 216.932	−246 530.3939	1 007 820.232	5 821 667.794
η_4 (eV)	−7 897 517.078	1 232 710.480	−5 039 078.186	−29 109 527.37
k	0.00	−0.03	−0.03	−0.05
r_m (Å)	4.28	9.14	5.21	4.55
A	291.209 481 3	$-2.859\,062\,644\times10^{-2}$	16.783 560 73	−606.371 212 0
d_1	−2.115 702 540	−1.134 902 214	−1.705 128 491	−2.054 768 934
d_2	1.860 194 164	0.510 640 043 2	1.202 678 444	1.745 919 130
d_3	−0.869 886 607 8	−0.119 020 209 7	−0.448 345 106 9	−0.784 664 821 8
d_4	0.228 202 300 3	$1.544\,861\,052\times10^{-2}$	$9.299\,515\,027\times10^{-2}$	0.196 528 667 7
d_5	$-3.185\,392\,442\times10^{-2}$	$-1.069\,924\,108\times10^{-3}$	$-1.015\,649\,285\times10^{-2}$	$-2.597\,366\,108\times10^{-2}$
d_6	$1.849\,148\,428\times10^{-3}$	$3.110\,346\,910\times10^{-5}$	$4.551\,740\,974\times10^{-4}$	$1.412\,876\,419\times10^{-3}$
β	10	10	10	10
α (Å^{-1})	13	8	16	12
b_1	−0.194 840 200 7	$8.328\,384\,243\times10^{-2}$	$3.285\,662\,172\times10^{-2}$	$-8.709\,497\,773\times10^{-2}$
b_2	$4.638\,911\,783\times10^{-2}$	$3.705\,566\,886\times10^{-2}$	0.103 800 838 3	0.179 414 316 9
	Na	Nb	Ni	Rb
γ_1 (eV)	68.306 100 04	−30 487.694 53	−205.057 080 3	649.849 283 7
γ_2 (eV)	730.074 629 0	−933 760.2020	−34 354.644 27	18 460.710 49
γ_3 (eV)	10 327.208 74	−12 442 153.00	−435 084.1284	246 548.8572
γ_4 (eV)	51 451.807 57	−62 212 159.16	−2 188 804.122	1 232 649.268
η_1 (eV)	16.831 351 09	31 724.570 69	1980.888 186	−582.806 865 3
η_2 (eV)	730.085 800 4	−933 760.4790	−34 352.415 57	18 460.710 97
η_3 (eV)	−10 262.669 88	12 442 751.74	439 300.9830	−246 513.6091
η_4 (eV)	51 456.267 44	−62 212 268.80	−2 187 917.470	1 232 649.467
k	0.00	−0.03	0.07	−0.02
r_m (Å)	7.33	4.84	4.44	8.60

TABLE II. (*Continued.*)

	Na	Nb	Ni	Rb
A	−0.145 780 869 3	−1018.281 136	91.324 540 26	−0.364 586 132 9
d_1	−1.477 709 511	−1.896 433 957	−2.161 849 925	−1.093 150 118
d_2	0.880 889 107 9	1.493 092 287	1.942 229 116	0.493 342 805 1
d_3	−0.274 186 820 6	−0.624 518 355 7	−0.927 081 647 3	−0.117 933 044 2
d_4	$4.737\,762\,157\times10^{-2}$	0.146 315 869 9	0.247 707 891 3	$1.577\,608\,797\times10^{-2}$
d_5	$-4.319\,465\,237\times10^{-3}$	$-1.819\,783\,364\times10^{-2}$	$-3.510\,205\,720\times10^{-2}$	$-1.120\,569\,879\times10^{-3}$
d_6	$1.622\,819\,249\times10^{-4}$	$9.382\,896\,316\times10^{-4}$	$2.059\,803\,146\times10^{-3}$	$3.307\,376\,507\times10^{-5}$
β	10	10	10	10
α (Å^{-1})	7	10	7	6
b_1	−0.134 888 221 8	0.143 696 528 0	0.326 573 273 1	$3.571\,735\,223\times10^{-3}$
b_2	$2.007\,174\,856\times10^{-2}$	−0.102 173 022 2	0.224 032 470 4	−0.102 145 935 8

IV. NUMERICAL RESULTS AND DISCUSSION

The EAM model parameters for the 12 metals are displayed in Table II. In Figs. 1–3, the theoretical pressure-volume curves reproduced by the models are compared with the experimental data of Ref. 34. For Fe (Fig. 3), these data extend to only about 0.05 Mbar, so experimental P-V data from other sources,[35] taken at higher pressure, are also shown, although no attempt was made to match the theoretical P-V relation for Fe to the higher-pressure data.

The theoretical phonon-frequency spectra, calculated from the formulas given by Ningsheng, Wenlan, and Chen[36] are compared with experimental data[37] in Fig. 4. There is generally good agreement between the theoretical and calculated phonon spectra, which indicates that the EAM models display reasonable lattice dynamics behavior. Among the metals represented, the bcc transition metals Mo and Nb have the most complex phonon spectra, and accordingly, the theoretical phonon spectra of these metals tend to show the greatest divergences from experiment. In both cases, however, the theoretical curves do capture important experimental features, although the fit is much better for Mo than for

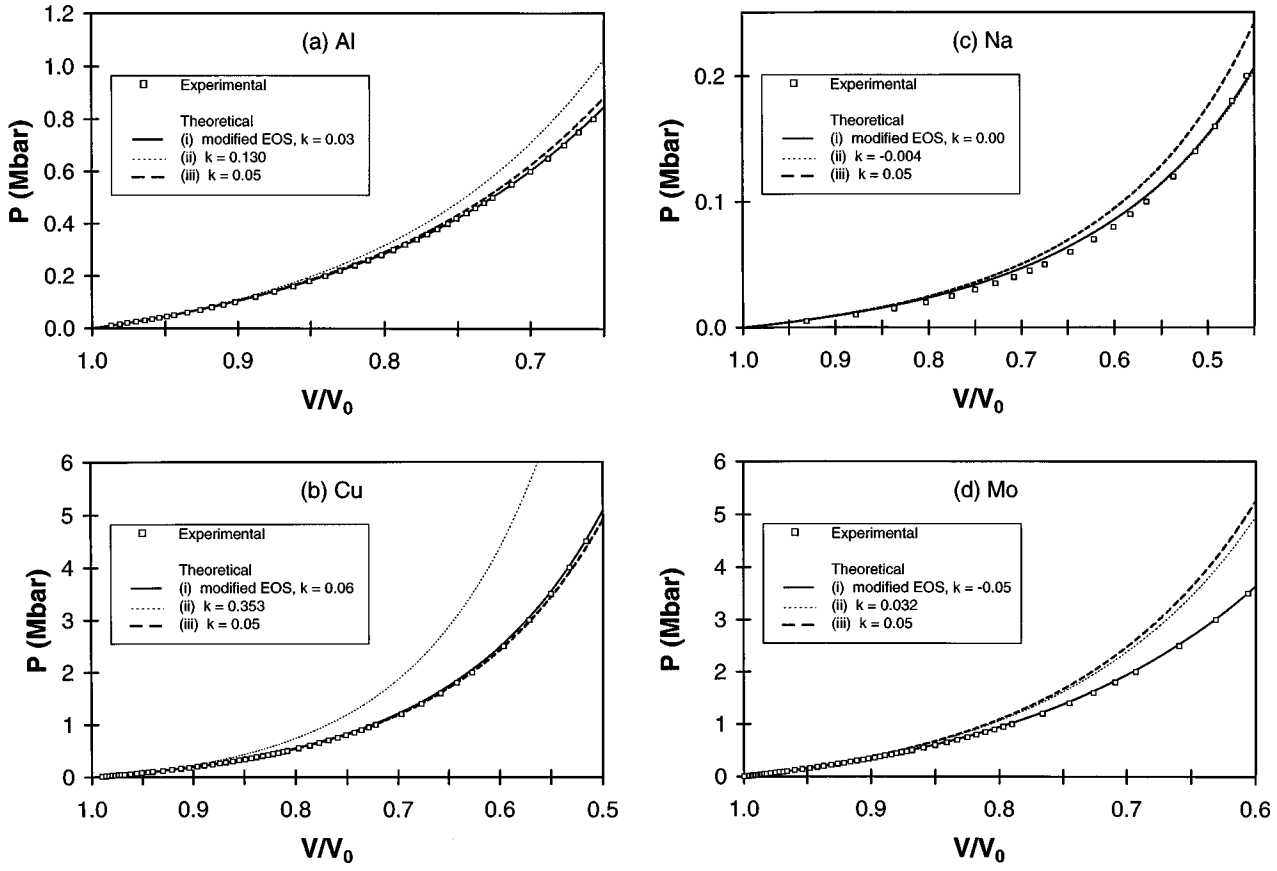

FIG. 1. Experimental and theoretical compression data of the metals (a) Al, (b) Cu, (c) Na, and (d) Mo. Experimental data (□) are from Ref. 34. The three theoretical curves are based on Rose's equation of state in which (i) the modification described by Eq. (9) is employed (solid line), (ii) Rose's equation is unmodified, with k determined from Eqs. (7) and (8) (dotted line), and (iii) Rose's equation is unmodified, with $k=0.05$ (dashed line).

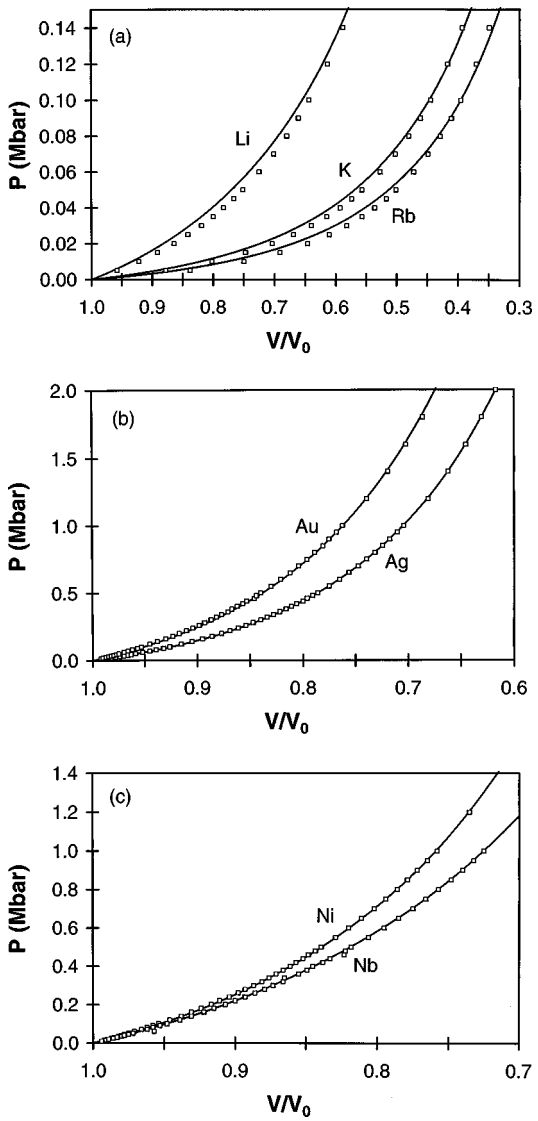

FIG. 2. Compression behavior (□, experimental; solid line, theoretical). (a) Li, K, and Rb. (b) Ag and Au. (c) Nb and Ni. Theoretical results employ the modified EOS described by Eq. (9).

Nb. The poorer agreement for Nb may be associated with a high degree of directional bonding in that metal, which is not fully reflected in the EAM model; this directional bonding apparently also causes Nb to have a very high shear modulus ratio $(C_{11}-C_{12})/2C_{44}$, when compared with other bcc metals.[38]

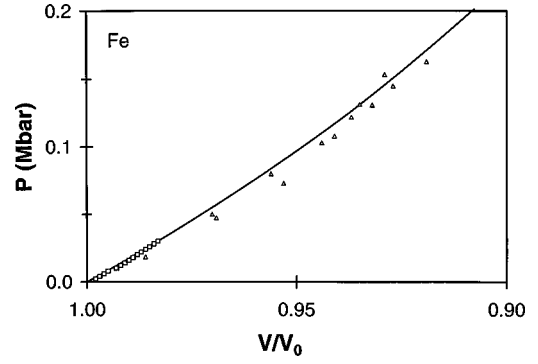

FIG. 3. Compression behavior for Fe [□, experimental (Ref. 34); △, experimental (Ref. 35); and solid line, theoretical].

The theoretical volumes and energies of the bcc and fcc structures of each metal at zero pressure are shown in Table III. These results are in accord with experimental phase stability observations. That is, among these metals, at zero pressure, the theoretical bcc structure is preferred to fcc for Fe, K, Mo, Nb, and Rb, and theoretically fcc is more favorable than bcc for the remaining metals. At low temperatures, the experimentally observed phases of the metals[33] are bcc for K, Fe, Mo, Nb, and Rb, fcc for Ag, Al, Au, Cu, and Ni, and close-packed structures that are similar to fcc with periodic stacking faults for Na and Li (such close-packed structures apparently differ little in energy from the fcc phase). The relative energetics of the EAM models for Li and Na, which are constructed using low-temperature bcc data, also agree with the prediction of pseudopotential models.[8]

Under increasing pressure, Na transforms to a bcc structure, and Fe, K, and Rb transform to fcc.[33] Table IV compares the theoretical pressures, where the differences between the free energies of the bcc and fcc structures vanish, and the experimental pressures, at which phase transitions occur for these metals. If conditions of local phase stability[8] are neglected, and the assumption is made that the transition should occur when $\Delta G=0$, then the result for Na is in best agreement with experiment. The model for K underpredicts the transition pressure by 27%, whereas the Fe and Rb models predict transition pressures that differ from experiment by factors of about 2 and 3, respectively.

Some final comments on the rationale that led to the present EAM models are perhaps in order. Characteristics that make any model attractive philosophically and/or useful practically include (i) simple analytic formulations, (ii) few empirical parameters, (iii) computational tractability, (iv) suitable theoretical foundations, and (v) good agreement between theory and experiment. However, the present ''state of the art'' of modeling the elastic properties of metals generally precludes incorporating all of these features. For example, pseudopotential models with but two empirical parameters can describe anisotropic, anharmonic, elastic properties of *simple* metals reasonably well,[39] but the analytic formulation is formidable and often unsuitable for use in molecular-dynamics simulations. Pseudopotential formulas for elastic moduli of even the second order, at finite strain, are complex [see Eqs. (A21) and (A37) in Ref. 39] and analytical expressions for the third-order moduli of pseudopotential models at finite strain apparently are not available. By contrast, these moduli (which are central to theories of stability and bifurcation in crystals under load[6–11,40]) are readily expressed analytically and computed in the EAM framework. In principle, EAM functions can be determined from first principles,[41] but in practice they are invariably determined semiempirically; various forms and fitting procedures have appeared in the literature,[13,42–46] although with the exception of the present work and Ref. 2, none has accurately modeled both the SOEM and the TOEM of metals. A common procedure is to determine the function parameters of some prespecified analytic forms by means of an optimization scheme (e.g., a nonlinear least-squares method) that minimizes the difference between calculated and experimental values of predetermined physical proper-

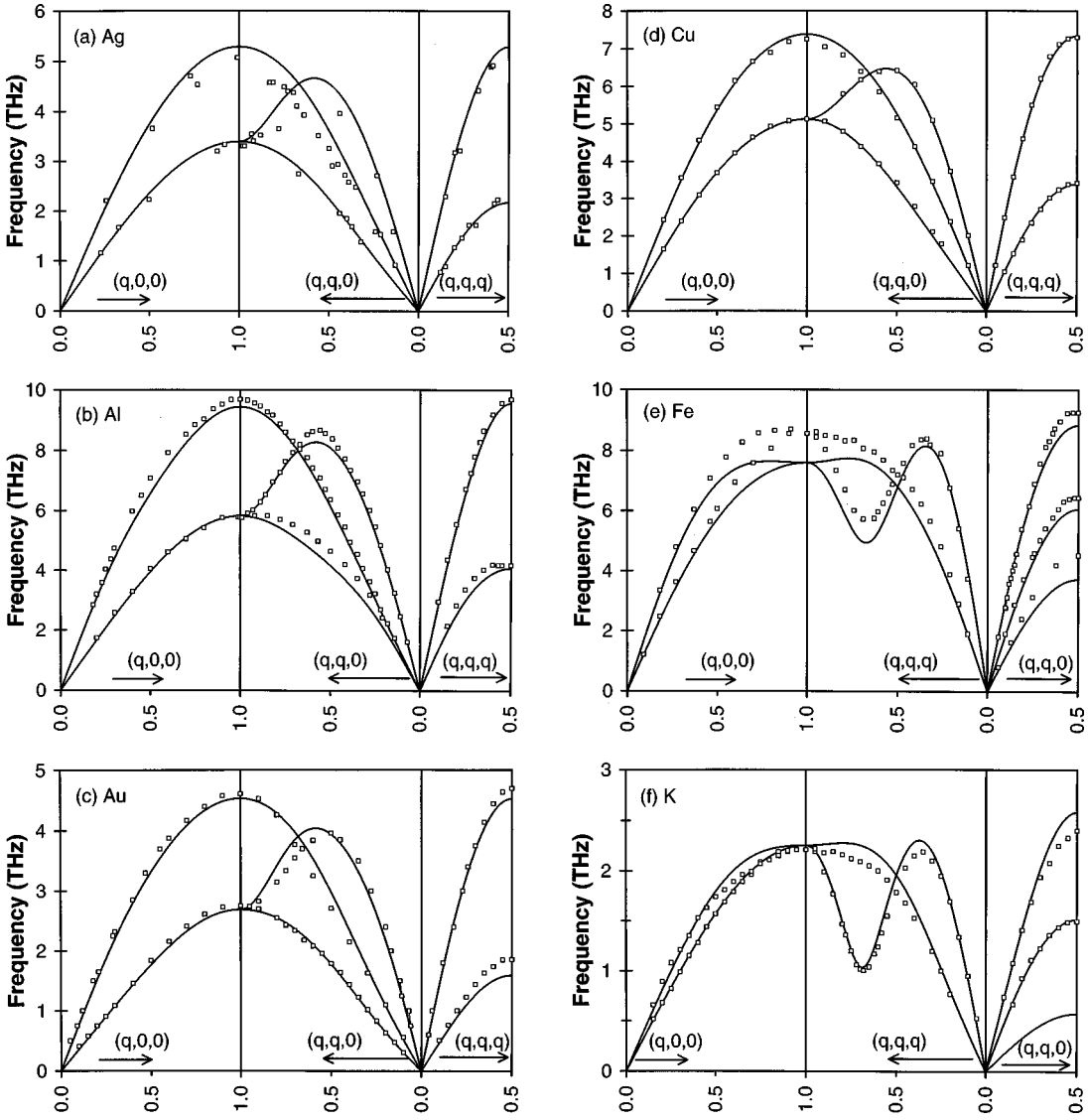

FIG. 4. Experimental and theoretical phonon-dispersion curves. Squares represent experimental data from Ref. 37; (a) Ag, (b) Al, (c) Au, (d) Cu, (e) Fe, (f) K, (g) Li, (h) Mo, (i) Na, (j) Nb, (k) Ni, and (l) Rb.

ties. Such a procedure reduces the required number of internal parameters; it was considered here, but not adopted, for the following reasons. Since an intended use of the present models is the exploration of finite strain elastic behavior, it is highly desirable that they yield appropriate values of the SOEM and TOEM. As shown in Ref. 2, EAM models can indeed exhibit accurate values for all of the SOEM and TOEM of cubic metals, provided that the pair potential ϕ satisfies six independent equations [Eqs. (24)–(29) in Ref. 2] and that the electron-density function f satisfies two additional independent equations [Eqs. (22) and (23) in Ref. 2]. Since EAM functions are often used in defect studies, it is customary to incorporate empirical values of unrelaxed vacancy energy, which, in the present case, adds a seventh relation for the pair potential to satisfy. The construction of a pair potential could then proceed either by selecting an analytic form with a sufficient number of internal parameters (i.e., a minimum of seven) to satisfy the requisite fundamental equations identically, or by selecting a form with fewer internal parameters, the values of which would be determined from an optimization procedure based on these seven equations. The latter procedure would be preferred if some fundamentally ''superior'' analytic form of ϕ were known; however, lacking such information, little is lost (in terms of simplicity and utility) by approximating ϕ as a series to the sixth power in r, with a cutoff employed to ensure rapid convergence of the lattice summations and continuity of the pair potential and its first three derivatives. As for the electron-density function, while a minimum of two empirical parameters are needed in principle, $f(r)$ must be oscillatory in general,[2] which suggests the use of a third, and a fourth is introduced to ensure rapid convergence; thus, apparently four is a ''practical'' minimum number of parameters in $f(r)$. With regard to the EOS used to determine the embedding function, while Rose's formulation, with but one adjustable parameter k, was found[2] to provide reasonably good pressure-volume relations, improved comparisons with experiment can be obtained, without great loss of simplicity, by employing a power series EOS functional at the lower magnitudes of pressure; no new data are required for this modification since this functional is matched to Rose's equation at intermediate pressure values and is determined from the elas-

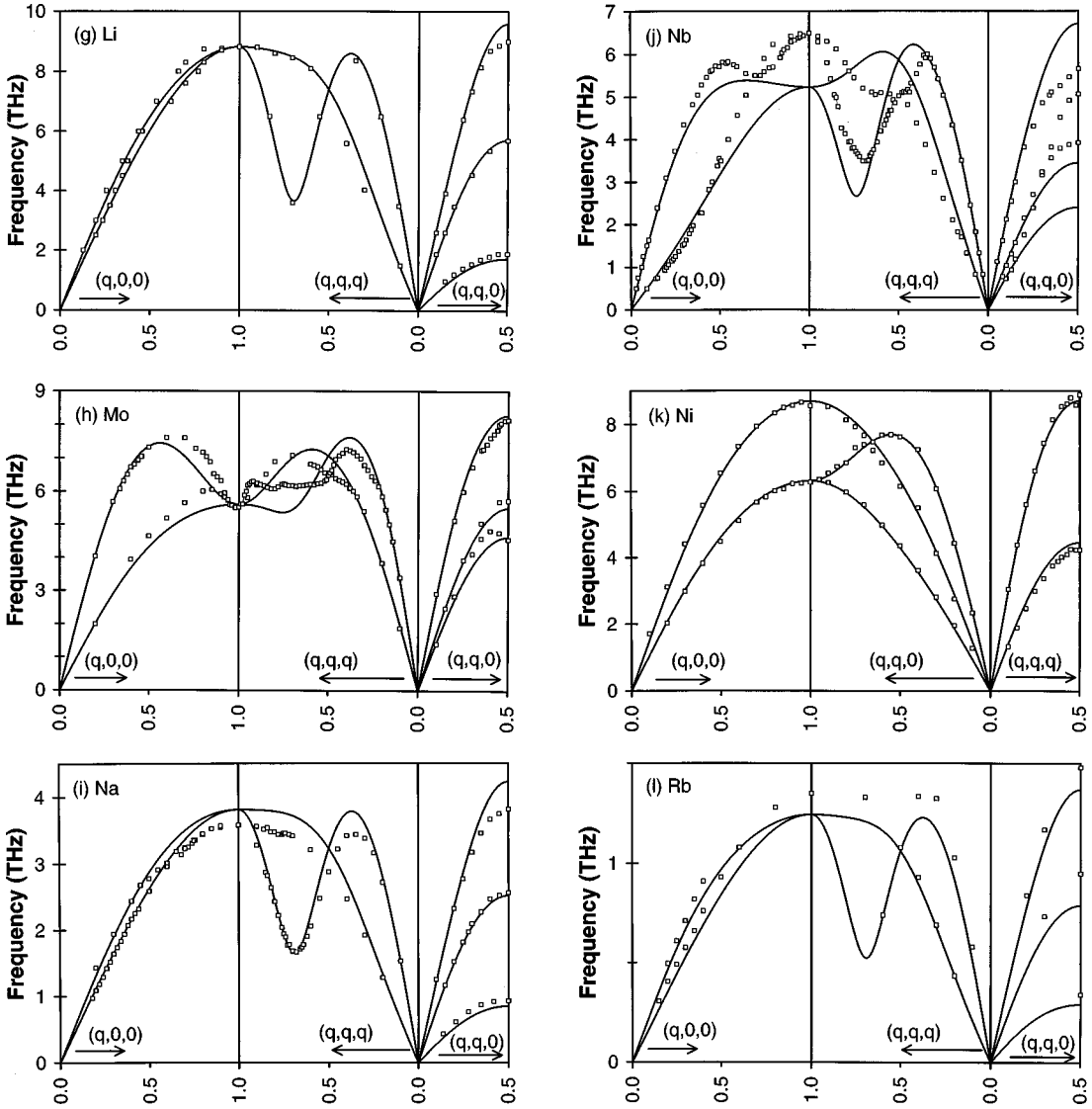

FIG. 4. (*Continued.*)

TABLE III. Theoretical lattice parameters (a), atomic volumes (V), and cohesive energies per atom (E) of the unstressed bcc and fcc structures of Ag, Al, Au, Cu, Fe, K, Li, Mo, Na, Nb, Ni, and Rb.

	a_{bcc} (Å)	V_{bcc} (Å^3)	E_{bcc} (eV)	a_{fcc} (Å)	V_{fcc} (Å^3)	E_{fcc} (eV)	$E_{fcc}-E_{bcc}$ (eV)
Ag	3.255	17.24	−2.9297	4.100	17.23	−2.9500	−0.0203
Al	3.220	16.69	−3.2608	4.030	16.36	−3.3400	−0.0792
Au	3.253	17.21	−3.7635	4.090	17.10	−3.8100	−0.0465
Cu	2.856	11.64	−3.4688	3.600	11.66	−3.5000	−0.0312
Fe	2.870	11.82	−4.2900	3.613	11.79	−4.2221	0.0679
K	5.250	72.35	−0.9410	6.631	72.89	−0.9402	0.0008
Li	3.490	21.25	−1.6500	4.443	21.93	−1.6610	−0.0110
Mo	3.150	15.63	−6.8100	4.151	17.88	−6.5086	0.3014
Na	4.230	37.84	−1.1300	5.337	38.00	−1.1302	−0.0002
Nb	3.310	18.13	−7.4700	4.291	19.75	−7.3424	0.1276
Ni	2.776	10.70	−4.3959	3.520	10.90	−4.4500	−0.0541
Rb	5.620	88.75	−0.8520	7.083	88.84	−0.8512	0.0008

TABLE IV. Comparison between the theoretical pressures (P_{theor}) where the differences between the free energies of the fcc and bcc structures ($\Delta G = G_{\text{fcc}} - G_{\text{bcc}}$) vanish and the approximate experimental pressures (P_{expt}) (Ref. 33) at which phase transitions occur.

	P_{theor} (Mbar)	P_{expt} (Mbar)
Fe	0.23	0.11
K	0.080	0.11
Na	1.5×10^{-3}	1.4×10^{-3}
Rb	0.017	0.05

tic moduli at zero pressure. Finally, it is important to mention that, while this procedure does incorporate a substantial number of empirical parameters, this in itself does not ensure an intrinsic ability to describe relevant physical phenomena. (Consider, e.g., that central force atomic models of cubic metals are unable to describe accurately even the three second-order elastic moduli C_{11}, C_{12}, and C_{44}, no matter how many parameters are employed, owing to the condition of Cauchy symmetry, $C_{12}=C_{44}$, inherent in the central force approximation. Even the addition of a volume-dependent energy term to a central force model, while removing Cauchy symmetry, still imposes physically unrealistic restrictions on the third-order elastic moduli.[47])

In summary, the EAM models that are developed here have a number of desirable features, such as (i) the linear and nonlinear elastic responses and the pressure-volume relations of the metals are accurately modeled, (ii) the quality of the phonon spectra ranges from ''very good'' to ''reasonably good'' (with the notable exception of Nb), (iii) the relative energetics between the unstressed bcc and fcc structures corresponds with experiment, and for Fe, K, Na, and Rb, experimentally observed phase transitions are indicated, (iv) the energy of the crystal and its derivatives are represented by convenient analytical forms, and (v) the lattice summations converge rapidly (generally after third- or fourth-nearest-neighbor interactions), so applications are not computationally intensive (the necessity of including at least third-nearest-neighbor interactions has been noted[2]). The present EAM models are thus quite suitable for various purposes, including Monte Carlo or molecular-dynamics simulations. As mentioned earlier, we intend, in due course, to use these models in a variety of crystal mechanics studies; the first of these appears in the following paper.

ACKNOWLEDGMENT

We wish to acknowledge the support of the Campus Laboratory Collaborations Program of the University of California.

*Present address: King Mongkut's University of Technology Thonburi, Bangkok 10140, Thailand.

[1] M. S. Daw, S. M. Foiles, and M. I. Baskes, Mater. Sci. Rep. **9**, 251 (1993).
[2] S. Chantasiriwan and F. Milstein, Phys. Rev. B **48**, 14 080 (1996).
[3] F. Milstein, Phys. Rev. B **3**, 1130 (1971).
[4] E. Esposito, A. E. Carlsson, D. D. Ling, H. Ehrenreich, and C. D. Gelatt, Jr., Philos. Mag. A **41**, 251 (1980).
[5] F. Milstein and B. Farber, Philos. Mag. A **42**, 19 (1980).
[6] R. Hill and F. Milstein, Phys. Rev. B **15**, 3087 (1977).
[7] F. Milstein, in *Mechanics of Solids*, edited by H. G. Hopkins and M. J. Sewell (Pergamon, Oxford, 1982), pp. 417–452.
[8] F. Milstein and D. J. Rasky, Phys. Rev. B **54**, 7016 (1996).
[9] F. Milstein and R. Hill, J. Mech. Phys. Solids **27**, 255 (1979).
[10] F. Milstein, J. Marschall, and H. E. Fang, Phys. Rev. Lett. **74**, 2977 (1995).
[11] F. Milstein, H. E. Fang, X. Y. Gong, and D. J. Rasky, Solid State Commun. **99**, 807 (1996).
[12] J. H. Rose, J. R. Smith, F. Guinea, and J. Ferrante, Phys. Rev. B **29**, 2963 (1984).
[13] S. M. Foiles, M. I. Baskes, and M. S. Daw, Phys. Rev. B **33**, 7983 (1986).
[14] P. B. Ghate, Phys. Rev. **139**, 1666 (1965).
[15] G. Simmons and H. Wang, *Single Crystal Elastic Constants and Calculated Aggregate Properties: A Handbook* (MIT, Cambridge, 1971).
[16] R. W. Balluffi, J. Nucl. Mater. **69&70**, 240 (1978).
[17] M. J. Fluss, L. C. Smedskjaer, M. K. Chason, D. G. Legnini, and R. W. Siegel, Phys. Rev. B **17**, 3444 (1978).
[18] L. De Schepper, D. Segers, L. Dorikens-Vanpraet, M. Dorikens, G. Knuyt, L. M. Stals, and P. Moser, Phys. Rev. B **27**, 5257 (1983).
[19] R. A. McDonald, R. C. Shukla, and D. K. Kahaner, Phys. Rev. B **29**, 6489 (1984).
[20] R. Feder, Phys. Rev. B **2**, 828 (1970).
[21] K. Maier, M. Peo, B. Saile, H. E. Schaefer, and A. Seeger, Philos. Mag. A **40**, 701 (1979).
[22] R. Feder and H. Charbnau, Phys. Rev. **149**, 464 (1966).
[23] W. Wycisk and M. Feller-Knipmeier, J. Nucl. Mater. **69&70**, 616 (1978).
[24] R. A. McDonald, R. C. Shukla, and D. K. Kahaner, Phys. Rev. B **29**, 6489 (1984).
[25] Charles Kittel, *Introduction to Solid States Physics*, 4th ed. (Wiley, New York, 1971), p. 96.
[26] Y. Hiki and A. V. Granato, Phys. Rev. **144**, 411 (1966).
[27] J. F. Thomas, Phys. Rev. **175**, 955 (1968).
[28] P. B. Powell and M. J. Skove, J. Appl. Phys. **56**, 1548 (1984).
[29] R. Srinivasan, J. Phys. Chem. Solids **34**, 611 (1973).
[30] F. F. Voronov, V. M. Prokhurov, E. L. Gromnitskaya, and G. G. Ilina, Fiz. Met. Metalloved. **45**, 1263 (1978) [Phys. Met. Metallogr. **45**, 123 (1978)].
[31] L. Graham, H. Nadler, and R. Chang, J. Appl. Phys. **39**, 3025 (1968).
[32] M. W. Riley and M. J. Skove, Phys. Rev. B **8**, 466 (1973).
[33] D. A. Young, *Phase Diagrams of the Elements* (University of California Press, Berkeley, 1991).
[34] *American Institute of Physics Handbook*, 3rd ed. (McGraw-Hill, New York, 1972).
[35] H. K. Mao, B. A. William, and T. Takahashi, J. Appl. Phys. **38**, 272 (1967); A. P. Jephcoat, H. K. Mao, and P. M. Bell, J. Geophys. Res. **91**, 4677 (1986).
[36] L. Ningsheng, X. Wenlan, and S. C. Chen, Solid State Commun. **69**, 155 (1989).
[37] *Metals: Phonon and Electron States, and Fermi Surfaces*, Group

III, Vol. 13a, Pt. a, edited by K. H. Hellwege and J. L. Olsen, Landolt-Börnstein, New Series (Springer, Berlin, 1981).
[38] F. Milstein and J. Marschall, Acta Metall. Mater. **40**, 1229 (1992).
[39] D. J. Rasky and F. Milstein, Phys. Rev. B **33**, 2765 (1986).
[40] R. Hill, Proc. Math. Camb. Philos. Soc. **92**, 167 (1982).
[41] M. S. Daw, Phys. Rev. B **39**, 7441 (1989).
[42] M. W. Finnis and J. E. Sinclair, Philos. Mag. A **50**, 45 (1984).
[43] R. A. Johnson, Phys. Rev. B **37**, 3924 (1988).
[44] R. A. Johnson and D. J. Oh, J. Mater. Res. **4**, 1195 (1989).
[45] J. B. Adams and S. M. Foiles, Phys. Rev. B **41**, 3316 (1990).
[46] Y. R. Wang and D. B. Boercker, J. Appl. Phys. **78**, 122 (1995).
[47] C. S. G. Cousins and J. W. Martin, J. Phys. F **8**, 2279 (1978).